

# Dalton Transactions

Accepted Manuscript



This is an *Accepted Manuscript*, which has been through the Royal Society of Chemistry peer review process and has been accepted for publication.

*Accepted Manuscripts* are published online shortly after acceptance, before technical editing, formatting and proof reading. Using this free service, authors can make their results available to the community, in citable form, before we publish the edited article. We will replace this *Accepted Manuscript* with the edited and formatted *Advance Article* as soon as it is available.

You can find more information about *Accepted Manuscripts* in the [Information for Authors](#).

Please note that technical editing may introduce minor changes to the text and/or graphics, which may alter content. The journal's standard [Terms & Conditions](#) and the [Ethical guidelines](#) still apply. In no event shall the Royal Society of Chemistry be held responsible for any errors or omissions in this *Accepted Manuscript* or any consequences arising from the use of any information it contains.

## ARTICLE

# Synthesis and Investigation of Cobalt Chalcogenide Clusters with Thienyl Phosphine Ligands as New Acceptor Materials for P3HT

Cite this: DOI: 10.1039/x0xx00000x

Received 00th January 2012,  
Accepted 00th January 2012

DOI: 10.1039/x0xx00000x

www.rsc.org/

B. J. Reeves<sup>a</sup>, D. M. Shircliff<sup>a</sup>, J. L. Shott<sup>a</sup>, and B. M. Boardman<sup>a\*</sup>,

Cobalt selenide clusters with 2-bromo-5-diethylphosphinothiophene (**1**) and 2-bromo-5-diphenylphosphinothiophene (**2**) ligands are described. The phosphine ligands are obtained via lithium halogen exchange of 2,5-dibromothiophene followed by addition of chlorodiethylphosphine and chlorodiphenylphosphine, respectively. The prepared phosphine ligands are then sequentially reacted with elemental selenium followed by dicobalt octacarbonyl to yield  $\text{Co}_6\text{Se}_8(\text{P}(\text{Et})_2(\text{C}_4\text{H}_2\text{SBr}))_6$  (**3**) or  $\text{Co}_6\text{Se}_8(\text{P}(\text{Ph})_2(\text{C}_4\text{H}_2\text{SBr}))_6$  (**4**), respectively. The two new cobalt selenide clusters were characterized by UV-visible spectroscopy, Fourier-transform infrared spectroscopy, cyclic voltammetry, and elemental analysis. Emission spectra were recorded for the addition of,  $\text{Co}_6\text{Se}_8(\text{PEt}_3)_6$  (**5**), **3**, and **4** to a 0.004 wt% solution of poly-3-hexyl thiophene (P3HT) in toluene to investigate the charge transport of the system. The quenching of the polymers' emission follows first-order like decay for each cluster. Clusters **3** and **4** are approximately twice as efficient at quenching the emission than cluster **5** with **4** being slightly more efficient than **3**. Simple mixtures of **3**, **4** or **5** and P3HT were spun cast from toluene into thin films and atomic force microscopy displayed relatively uniform dispersion of **3** and network-like formation of **4** in contrast to the phase separation of **5** in the polymer films.

## Introduction

The bulk hetero-junction (BHJ) photovoltaic architecture is applicable to a wide variety of materials and recently conjugated polymers and inorganic semiconductor nanoparticle systems have been developed to obtain hybrid structures.<sup>1,2,3,4,5</sup> These types of hybrid materials have also found applications in many areas of technology such as memory devices,<sup>6,7</sup> light-emitting diodes,<sup>8,9</sup> and catalysis.<sup>10</sup> Additionally, they are advantageous for organic photovoltaic (OPV) applications because they combine the strong light harvesting capabilities of the inorganic component with the ability to solution process well-ordered structures for efficient charge separation and migration of the organic component. Colloidal semi-conducting nanocrystals or nanoparticles are often used as the inorganic component in these types of devices. Nanoparticles are of interest in energy conversion and light harvesting applications because of their size-tunable IR band gaps and solution processability.

Hybrid materials formed by incorporating nanoparticles into organic conjugated molecules often display interesting properties. For example many hybrid structures are made with poly-3-hexylthiophene (P3HT) and inorganic nanoparticles.<sup>3,11,12,13</sup> Incorporation of gold nanoparticles into polypyrrole,<sup>14</sup> polyaniline,<sup>15</sup> and polythiophene<sup>16</sup> films have displayed an increase of two orders of magnitude in the conductivity when compared to the pure polymer films. While there has been some success with these materials, they are plagued by a few fundamental problems. It has been previously reported that the efficiency of these types of devices depends heavily on the percolation of the network of inorganic and organic material for electron and hole extraction.<sup>17,18</sup> Generally, mixing leads to an aggregation of the inorganic particles rather than the preferred dispersion throughout the polymer. In a few cases, dispersion of inorganic particles has been achieved; however, a coating on the inorganic particle was necessary to achieve increased solubility and stability for favorable interaction.<sup>19,20,21,22</sup> In these cases, the coating makes it difficult to understand the direct chemical interactions between the two materials.<sup>23</sup> Additionally, it is often difficult to prepare nanoparticles with a narrow distribution of particle size. This is important when dealing with BHJ devices because of the exciton diffusion length (10nm)<sup>24,25</sup>; if the particles are too large, or there are large aggregates of nanoparticles, it is difficult to get enough donor/acceptor interfacial interactions.

There has been considerable interest in phosphine chalcogenides for their uses as sulfur and selenium transfer agents as well as building blocks to understand the formation of bulk metal chalcogenides.<sup>26,27,28</sup> These studies have allowed for a better understanding of the growth of extended metal chalcogenide

<sup>a</sup> Department of Chemistry and Biochemistry MSC 4501, James Madison University, Harrisonburg, VA 22807.

†Electronic Supplementary Information (ESI) available: Synthesis and characterization of phosphine ligands, powder X-ray data, UV-visible and fluorescence spectra, and electrochemical data; figures (Fig S1-7) See DOI: 10.1039/b000000x/

semiconducting solids,<sup>27,28</sup> as well as understanding the role of phosphine chalcogenides in the synthesis and properties of colloidal quantum dots.<sup>29,30</sup> Functionalized phosphines have exhibited increasing potential for use in a number of applications ranging from catalysis to biomedical.<sup>31,32,33</sup>

Recently, thiophene-containing phosphines have been synthesized and incorporated into tungsten sulfide clusters through ligand exchange reactions.<sup>34</sup> The thienyl moieties provide an interesting opportunity to covalently link metal chalcogenide clusters to conjugated polymers reducing the non-favorable interactions between the organic and inorganic materials. Unfortunately to date the electropolymerization of the attached thiophene moieties have proven unsuccessful due to over oxidation of the metal core.<sup>34</sup> Additionally, trialkyl phosphine chalcogenides have been used to isolate cobalt chalcogenide clusters with the formula type  $\text{Co}_6\text{Q}_8(\text{PR}_3)_6$  (Q= S, Se, or Te, R= ethyl, butyl).<sup>27,28</sup> This direct synthesis can be used to obtain new clusters with functionalized ligands. The resulting clusters are relatively robust to ambient conditions, soluble in common organic solvents, and have previously been shown to be conductive.<sup>35</sup> In addition to a broad absorption range, these properties give them the potential for use in a variety of materials applications.

In an effort to achieve a covalently linked organic-inorganic structure, two new ligands were developed. Herein we describe the synthesis of 2-bromo-5-diethylphosphinothiophene (**1**) and 2-bromo-5-diphenylphosphinothiophene (**2**). The synthesis of two cobalt selenide clusters  $\text{Co}_6\text{Se}_8(\text{P}(\text{Et})_2(\text{C}_4\text{H}_2\text{SBr}))_6$  (**3**) and  $\text{Co}_6\text{Se}_8(\text{P}(\text{Et})_2(\text{C}_4\text{H}_2\text{SBr}))_6$  (**4**) is also detailed. Unlike previous attempts, the bromine at the 2-position of the thiophene moiety provides options for milder polymerization conditions such as Grignard metathesis or palladium catalyzed polymerization.<sup>36</sup> Furthermore, we describe the spectroscopic study of the interactions between  $\text{Co}_6\text{Se}_8(\text{PEt}_3)_6$  (**5**), **3**, and **4** and P3HT. The charge transfer from the polymer donor to the cluster acceptor is observed in solution via photoluminescence quenching of P3HT. We also report on the importance of R-group substituents on the clusters interactions with the polymer and the morphology of the thin films by atomic force microscopy (AFM) analysis to understand the role of  $\pi$ -conjugated thiophene containing clusters in donor/acceptor applications.

## Experimental

### Materials and Instrumentation

All manipulations were performed under inert atmosphere using standard glovebox and Schlenk techniques, unless otherwise noted. Chlorodiethylphosphine (90%), chlorodiphenylphosphine (99%), 2,5-dibromothiophene (95%), and *n*-butyllithium (2.5 M in hexanes) were used as received from *Sigma-Aldrich*. Dicobalt octacarbonyl (stabilized in 1-5% hexanes) and selenium powder (99.5%) were used as received from *Strem Chemical*. The ligands 2-bromo-5-diethylphosphinothiophene (**1**) and 2-bromo-5-diphenylphosphinothiophene (**2**) were synthesized using a modified literature procedure and details can be found in the supplementary information.<sup>38</sup> The cluster  $\text{Co}_6\text{Se}_8(\text{PEt}_3)_6$  (**5**) and P3HT were synthesized according to literature procedures.<sup>35,37</sup> All solvents were obtained from an Innovative Technology Solvent Purification System and were degassed before use. Nuclear magnetic resonance (<sup>1</sup>H NMR and <sup>31</sup>P NMR) spectra were obtained using a Bruker Advance DPX-400 or 300 NMR spectrometer; chemical shifts are reported in ppm downfield from tetramethylsilane ( $\delta$  scale) and 85 %

$\text{H}_3\text{PO}_4$  respectively. FT-IR spectra were obtained using an Thermo Nicolet 380 FT-IR with SMART Golden Gate using EZ OMNIC 6.1a. UV-Visible spectra were taken in toluene and recorded using an HP 8453 Diode Array. Photoluminescence spectra were obtained on a Jasco FP-8500 spectrofluorometer using an excitation wavelength of 413 nm. Galbraith Laboratories performed elemental analysis. Microwave reactions were performed in a Biotage Initiator+ microwave synthesizer. AFM was performed on a Nanoscience Instruments Nanosurf AFM in tapping mode. Powder X-Ray diffraction data was collected on a PANalytical X'Pert PRO MPD theta-theta Diffractometer. Cyclic Voltammetry was performed on a CH Instruments CHI700D Electrochemical Analyzer. Polymer and polymer:cluster films were spun cast using a Best Tools Smart Coater SC100

### Preparation of $\text{Co}_6\text{Se}_8(\text{P}(\text{Et})_2(\text{C}_4\text{H}_2\text{SBr}))_6$ (**3**)

Elemental selenium (0.313 g, 3.966 mmol) was added to a solution of 2-bromo-5-diethylphosphinothiophene (0.498 g, 1.983 mmol) in toluene (4 mL) and heated to 160 °C for 10 minutes in the microwave. The reaction mixture was allowed to cool to room temperature and was subsequently filtered into a round bottom flask to remove excess selenium. Dicobalt octacarbonyl (0.156 g, 0.456 mmol) was dissolved in toluene (20 mL) and cannula transferred into the solution. The reaction turned a dark red/brown immediately and was allowed to stir at room temperature for 30 minutes and then heated to reflux overnight. The resulting dark red/black solution was cooled to room temperature, Schlenk filtered and concentrated to ~1 mL. The solution was stored in a freezer (-13 °C) over several days to afford deep red needles. The mother liquor was removed and the crystals were washed with cold diethyl ether and dried under vacuum to yield a very dark black/red solid (0.179 g, 47.2%). NMR <sup>31</sup>P (d-toluene): 60.6 (br).  $\lambda_{\text{Abs}}=366, 442, 502$  nm. IR (KBr,  $\text{cm}^{-1}$ ): 2951, 2953, 2919, 2864 (C-H), 1727 (aromatic C=C) *Anal. Calc* for  $\text{Co}_6\text{Se}_8\text{P}_6\text{C}_{48}\text{H}_{72}\text{S}_6\text{Br}_6$ : C, 23.13; H, 2.91; P, 7.46. Found: C, 23.56; H, 3.14; P, 7.12%.

### Preparation of $\text{Co}_6\text{Se}_8(\text{P}(\text{Ph})_2(\text{C}_4\text{H}_2\text{SBr}))_6$ (**4**)

Elemental selenium (0.227 g, 0.288 mmol) was added to a solution of 2-bromo-5-diphenylphosphinothiophene (0.500 g, 1.44 mmol) in toluene (4 mL) and allowed to react at 160 °C for 10 minutes in the microwave. The reaction mixture was cooled to room temperature and solution was filtered into a round bottom flask to remove excess selenium. Dicobalt octacarbonyl (0.114 g, .332 mmol) in 20 mL of toluene was subsequently cannula transferred into the reaction mixture. Rapid color change to dark red brown was observed, in addition to evolution of CO. The reaction mixture was allowed to stir at room temperature for 30 minutes followed by reflux overnight. The resulting deep red brown solution was Schlenk filtered and excess toluene was reduced to 1 mL in vacuo and stored in a freezer overnight (-13 °C). The mother liquor was removed and the resulting solid was washed with cold diethyl ether to yield a very dark black/red solid (0.113 g, 33%). NMR <sup>31</sup>P (d-toluene): 57.9 (br).  $\lambda_{\text{Abs}}=366, 447, 514$  nm. IR (KBr,  $\text{cm}^{-1}$ ): 3054, 3045, 2972, 2849 (C-H), 1807, 1760 (aromatic C=C) *Anal. Calc* for  $\text{Co}_6\text{Se}_8\text{P}_6\text{C}_{96}\text{H}_{72}\text{S}_6\text{Br}_6$ : C, 37.58; H, 2.36; P, 6.05. Found: C, 37.13; H, 2.37; P, 5.87%.

### Quenching Experiments

The emission quenching experiments were performed by the addition of 1.0 mg increments of **3**, **4**, or **5** to a 0.004 wt% solution of P3HT in toluene. The addition of each cluster was continued until negligible emission from the polymer was observed. The molecular

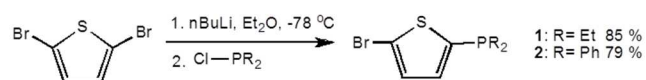
weight of P3HT (~13,000) was determined on a Polymer Labs GPC-50 Plus in THF using polystyrene standards.

## AFM

Cluster:P3HT films were spun-cast on untreated glass substrates from a toluene solution of 0.02 wt % P3HT and 0.12 wt% cluster at 1500 rpm and dried under vacuum. AFM images were recorded in tapping mode. The films were then annealed at 150 °C for 5 minutes and cooled rapidly to room temperature, AFM experiments were then repeated.

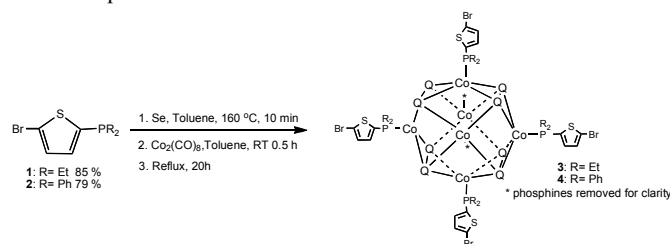
## Results and discussion

The tertiary thienyl phosphine ligands were synthesized by means of a modified literature procedure.<sup>38</sup> In each case, dibromothiophene was lithiated and then quenched with chlorodiethylphosphine or chlorodiphenylphosphine, to afford 2-bromo-5-diethylphosphinothiophene (**1**) and 2-bromo-5-diphenylphosphinothiophene (**2**), respectively (Scheme 1). Despite taking precautions to remove moisture and oxygen, a small amount of the phosphine oxide formed but was easily removed by column chromatography to afford the ligands in good yield.



**Scheme 1.** Synthesis of ligands **1** and **2**.

Clusters **3** and **4** were synthesized by reaction of a freshly prepared phosphine selenide with dicobalt octacarbonyl (Scheme 2). This reaction can be performed as a one pot synthesis by refluxing the phosphine ligand with excess selenium powder for 5 hours and then adding the dicobalt octacarbonyl via cannula. The phosphine selenide can also be isolated and combined with a solution of dicobalt octacarbonyl; however, the formation of the phosphine selenide in a microwave reactor is considerably more rapid, and hence the preferred method.



**Scheme 2.** Synthesis of clusters **3** and **4** via the in situ formation of the tertiary phosphine chalcogenide using microwave assisted synthesis and subsequent reaction with dicobalt octacarbonyl.

The <sup>31</sup>P NMR of **3** and **4** show broad peaks at 60.6 ppm and 57.9 ppm respectively. The shifts are downfield from ligands **1** and **2** (-21.8 ppm and -17.9 ppm) and are in agreement with previously published clusters with similar structures.<sup>39</sup> Characterization by UV-visible spectroscopy revealed three strong absorption bands for each cluster. The absorption spectra of the new clusters compare well with previous clusters as they share the three characteristic absorption bands of a cobalt chalcogenide cluster with the formula

type Co<sub>6</sub>Q<sub>8</sub>(PR<sub>3</sub>)<sub>6</sub> (Q = S, Se, or Te, R = ethyl, butyl) (Figure 1).<sup>27,28</sup> Co<sub>6</sub>Se<sub>8</sub>(PEt<sub>3</sub>)<sub>6</sub> (**5**) was synthesized according to the literature for comparison.<sup>35,39</sup> Interestingly, the first bands are comparable, while the second and third bands of the new clusters are slightly red shifted. This can likely be attributed to the increased conjugation of the thiophene-containing ligands. Infrared spectroscopy confirmed the absence of residual carbonyl, which indicates the consumption of the starting material (Co<sub>2</sub>CO<sub>8</sub>).

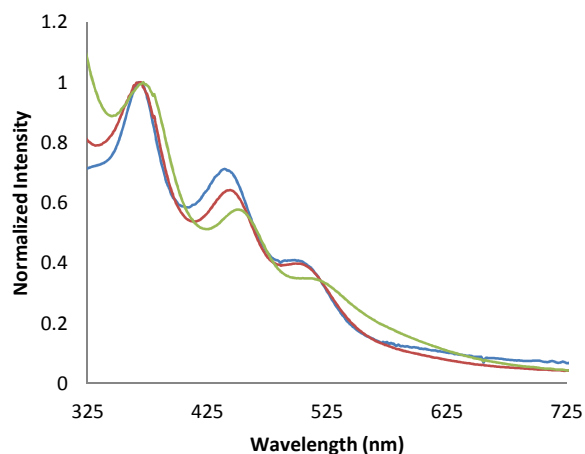


**Figure 1.** UV-visible absorption spectral overlay of the alkyl phosphine containing cluster and the thienyl phosphine containing clusters. Ligand 1=PEt<sub>3</sub> (blue), Ligand 2=PEt<sub>2</sub>ThBr (red), Ligand 3=PPh<sub>2</sub>ThBr (green).

To date, neither the telluride or sulfide clusters have been synthesized with the thienyl phosphine ligands. In order to understand this, many attempts were made to isolate the phosphine tellurides with no success. Mechanistically, in order for the cluster reaction to proceed, the phosphine chalcogenide must form first. In the case of the sulfide cluster, the phosphine sulfide forms rapidly and can be isolated with ease. However, due to the strength of the phosphine sulfide bond, when reacted with dicobalt octacarbonyl, it is likely that the oxidative addition of the bromothiophene moiety is the preferred reaction rather than the formation of the cluster. We recently reported the synthesis of thienyl phosphines with isopropyl R groups. Attempts to incorporate these ligands into cobalt chalcogenide clusters have also proven challenging. This is potentially due to the steric hindrance of the isopropyl groups. Unfortunately, NMR did not provide insight as to the structure of the products that were formed and single crystals have yet to be isolated from the above stated reactions. The UV-visible spectra were inconsistent with the spectra of previous clusters.

It is interesting to note that the ligands fluoresce similarly to thiophene itself, while the clusters that contain these ligands do not exhibit any significant fluorescence. For example, **1** has a  $\lambda_{Abs}$  at 293 nm with a red shifted  $\lambda_{Em}$  at 366 nm and 527 nm, while **3** does not exhibit any fluorescence (Figures S3 and S4). This suggests that cluster **3** is behaving as an acceptor and quenching the fluorescence of the thiophene moiety; **4** exhibits the same effect.

Considering the observed quenching, these clusters have considerable potential as acceptors to thiophene-containing donors such as P3HT. To further investigate this, cyclic voltammetry (CV) was performed for each of the clusters. The CV for **3** shows one reversible oxidation and two non-reversible reduction peaks while **4** has one reversible oxidation peak and two reversible reduction peaks (Figure S1 and S2). The oxidation potential from the CV can be used to calculate the energy of highest occupied molecular orbital (HOMO) of the clusters using the formula  $\text{HOMO} = -(E_{\text{ox}} - E_{\text{Ref}}) - 4.80$  with ferrocene/ferrocenium oxidation as the reference. The calculated HOMO levels are in agreement with previously published clusters (Figure 2).<sup>35,39</sup> The onset of absorption can be used to determine the energy gap between the HOMO and lowest unoccupied molecular orbital (LUMO) of the cluster. The energy levels are very important when considering these materials as acceptors in organic inorganic devices. Optimal energy level overlap of the polymer donor and the acceptor requires the LUMO of the acceptor to be lower in energy than the LUMO of the donor as depicted for P3HT and phenyl-C61-butyric acid methyl ester (PCBM) (Figure 2). While two of the clusters (**3** and **5**) exhibit LUMO energy levels slightly above that of P3HT, **4** has a slightly lower LUMO level of 2.79 eV giving it the greatest possibility to act as an acceptor with P3HT (Figure 2). Additionally all three clusters have a LUMO energy level that are significantly higher than that of PCBM. This increase is a key advantage of these materials because the maximum open circuit voltage ( $V_{\text{oc}}$ ) of devices is measured by the energy difference of the HOMO of the donor and the LUMO of the acceptor. For example a **4**:P3HT device could exhibit a  $V_{\text{oc}}$  as high as 1.97 eV where as a PCBM:P3HT device would only have a  $V_{\text{oc}}$  of 0.85 eV according to this energy diagram (Figure 2).

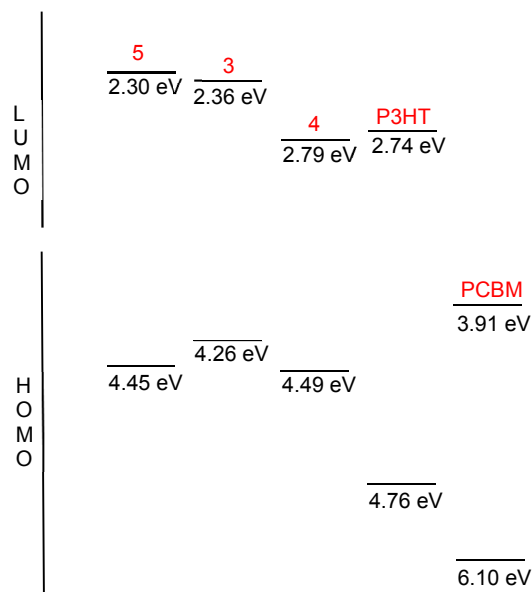


**Figure 2.** HOMO and LUMO energy levels of the clusters compared to those of P3HT<sup>40,41</sup> and PCBM<sup>40,42</sup>.

Solutions of each cluster and P3HT were prepared in a 1:7.5 P3HT to cluster ratio. The absorption of the cluster-polymer blends lie between the absorption of the pure cluster and polymer, indicating

that there is mixing of the two materials. A donor-acceptor type relationship between the clusters and the polymer is indicated by the combination of the two pure absorption spectra (Figure 3-top). Slight differences can be observed in the blend absorption spectra, which implies subtle difference in interactions between **3**, **4**, and **5** with P3HT based on the difference in R groups between the three clusters. To investigate the electronic interactions of the clusters and P3HT, fluorescence quenching experiments were performed. P3HT (0.004 wt % in toluene) was excited at 413 nm and an emission peak was observed at 555 nm. In separate experiments, each cluster (**3**, **4**, and **5**) were added in 1.0 mg increments to the polymer solution. The mixtures were sonicated to ensure completely homogeneous solutions and a fluorescence spectrum was taken after each addition. The data collected for P3HT with each cluster indicates charge transfer from the polymer donor to the cluster acceptor (Figure 3-bottom). In each experiment a significant reduction in the emission of the P3HT is observed after only 1.0 mg addition of **3**, **4**, or **5** (Figure S5).

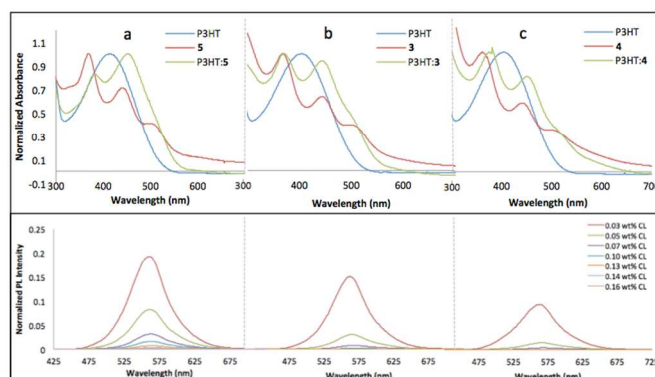


**Figure 3:** Top: UV-Vis absorption spectra of a) P3HT, **5**, and P3HT:**5**, b) P3HT, **3**, and P3HT:**3** and c) P3HT, **4**, and P3HT:**4**. All solutions were made in toluene with a 1:7.5 P3HT to cluster ratio. Bottom: Photoluminescence spectra of P3HT with addition of clusters **5** (a), **3** (b), and **4** (c). All solutions were prepared in toluene. (Normalized emission of P3HT was removed for clarity, full data including these spectra can be found in Figure S5.)

This reduction of the fluorescence indicates a transfer of the excited electron in the LUMO of the polymer to the LUMO of the cluster, suggesting acceptor-donor type interactions between the two materials. However, there is a clear difference in the ability of **4** to quench the polymer emission versus **5** (Figure 3a and c). Nearly complete reduction of the polymers fluorescence is observed after 0.05 wt% **4** has been added where as 0.13 wt % **5** is required before complete quenching is observed.

A first-order like decay of the polymer's fluorescence was observed for each polymer-cluster quenching experiment. A plot of the  $\text{Ln}(\text{Emission Intensity})$  vs weight % cluster shows a clear linear trend (Figure 4). P3HT's fluorescence was quenched efficiently with **3**, **4**, or **5** with decay values of 41.3 ( $\text{Ln}(\text{EmInt})/\text{wt}\%$  **5**), 73.2 ( $\text{Ln}(\text{EmInt})/\text{wt}\%$  **3**), and 94.1 ( $\text{Ln}(\text{EmInt})/\text{wt}\%$  **4**) respectively. Cluster **5** had the least efficient electron transfer by a factor of two compared to **3** or **4**. The increased LUMO energy of Clusters **5** (LUMO: 2.30 eV) and **3** (LUMO: 2.36 eV) could contribute to the lower efficiency of electron transfer from the polymer. As expected

from the lower LUMO energy with respect to P3HT, Cluster 4, shows the most efficient electron transfer. (Figure 2).

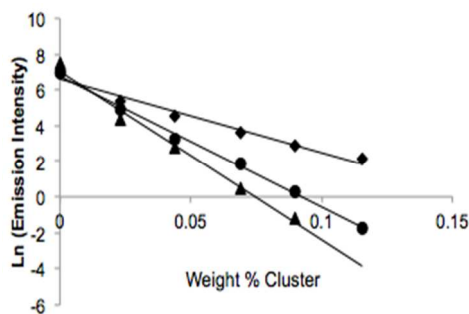


**Figure 4:** First-order type emission decay plots of 0.004 wt% P3HT in toluene with **5** (♦), **3** (•), and **4** (▲).

It has been well documented that these types of donor-acceptor interactions depend heavily on the interfacial interaction of the organic and inorganic components.<sup>13,17</sup> Cluster **5** has triethylphosphine ligands on the axial positions which should have minimal favorable interactions with the polymer. Clusters **3** and **4** each contain thienyl substituents on the axial phosphines and they both have very similar quenching efficiencies for P3HT. This observation suggests that the thienyl ligands on the cluster facilitate favorable interactions between the polymer backbone and the cluster. Cluster **3** contains two ethyl groups whereas **4** has two phenyl groups in addition to the thienyl moiety. The increased fluorescence decay rate observed with **4** could be attributed to increased  $\pi$ - $\pi$  interactions from the phenyl groups on the cluster with the P3HT backbone.

In addition to optimal orbital overlap, donor-acceptor interactions are very important in bulk heterojunction (BHJ) device architectures.<sup>43,44</sup> These interactions are very difficult to obtain due to the orthogonal solubility of most organic polymers and inorganic particles. In the case of these clusters and P3HT, there is a common solubility in tetrahydrofuran as well as toluene. Additionally, the thiophene moiety supplies an extra opportunity for interaction with polymers like P3HT through  $\pi$ - $\pi$  stacking. To illustrate this interaction with P3HT, AFM images of P3HT:**3** and P3HT:**4** were obtained (Figure 5: C and D). AFM images of P3HT and P3HT:**5** are shown for comparison to the new clusters (Figure 5: A and B). P3HT:**5** exhibits random phase separation of the cluster and polymer due to the non-complimentary interactions of the organic and inorganic components similar to those observed with traditional nanoparticles in polymer films. Visual comparison illustrates that **3** displays good dispersion throughout the polymer film. This can be attributed to the thienyl moiety, which leads to more  $\pi$ - $\pi$  stacking with P3HT and an increase in the interaction between the cluster and the polymer.

Favorable interaction between P3HT and **3** also contribute to the decreased surface roughness (RMS = 0.94 nm) compared to P3HT:**5**

which displayed a much higher a RMS value of 1.4 nm when compared to pure P3HT (RMS = 0.73). P3HT:**4** does not exhibit the same dispersion through the polymer film as is observed for P3HT:**3**, instead the as cast film has a network-like structure. The increased intermolecular interactions between the clusters also contribute to the slightly higher RMS value of 1.2 nm as opposed to **3**.

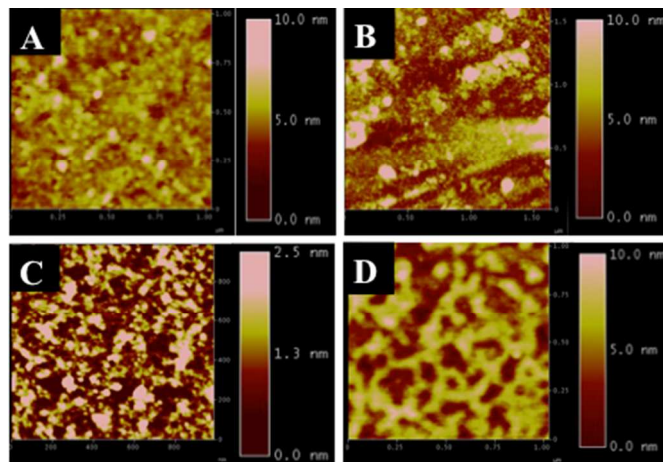


**Figure 5.** Topographical AFM images of (A): pure P3HT film; (B): P3HT:**5** film; (C): P3HT: **3** film; (D): P3HT: **4** film.

The ability of the axial ligands of **3** and **4** to facilitate the formation of ordered structures was further probed by AFM by collecting the phase image of both the as cast films and films that were annealed at 150 °C for 5 minutes. The phase images of the as cast films of P3HT:**5** and P3HT:**3** (Figure 6: A and B) show a clear difference in phase separation between the two films.

Large aggregates of **5** are observed while **3** displays even dispersion throughout the film. Similarly to P3HT:**3**, P3HT:**4** shows an even dispersion of **4** throughout the film (Figure 6: B and C), this correlates well with the fluoresce decay data indicating that the most favorable interactions and the most efficient electron transfer occurs between P3HT and **4**. After thermal annealing, minimal changes are observed for the P3HT:**5** (Figure 6: A and D) film however, a drastic difference is observed between P3HT:**3** (Figure 6 E) and P3HT:**4** (Figure 6 F). The annealed P3HT:**4** (Figure 6 F) film shows the formation of highly ordered network-like structures. The network-like structure of the film can be attributed to the phenyl rings of the ligand, inducing  $\pi$ - $\pi$  stacking between the clusters themselves as well as with the P3HT backbone. These results indicate **4** has the ability to not only act as an acceptor but also to form ordered structures, increasing the ability for hole transport in BHJ devices by combining both the  $\pi$ - $\pi$  stacking of the thienyl moiety which increases the interaction with the polymer and the  $\pi$ - $\pi$  stacking of the phenyl ligands.<sup>45</sup>

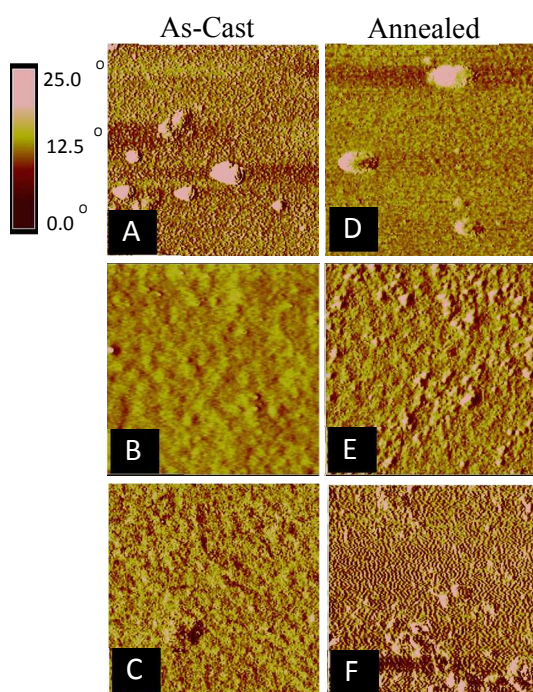


**Figure 6:**  $1\ \mu\text{m} \times 1\ \mu\text{m}$  tapping mode AFM phase images of as cast (left) and annealed (right) of P3HT:5 (A and D), P3HT: 3 (B and E), and P3HT:4 (C and F). Films were spun cast from a toluene solution of 0.02 wt % P3HT and 0.12 wt% cluster.

## Conclusions

Two new thiophene-containing phosphine ligands have been synthesized and isolated in good yields. In addition to the new ligands, two new cobalt selenide clusters containing the functionalized ligands have been synthesized and isolated. The formation of the sulfide and telluride clusters has proven unsuccessful to date due to the potential for oxidative addition of the bromothiophene moiety. Cyclic voltammetry suggests that these new clusters have good potential as inorganic acceptors to polymer donors because of their HOMO-LUMO levels when compared to the donor polymer P3HT. Additionally the increased energy of the LUMO levels provides the opportunity for a significant increase in the  $V_{oc}$  compared to that of PCBM, which would lead to significantly higher power conversion efficiency in bulk heterojunction devices.

Quenching experiments performed with cobalt clusters 3, 4, and 5 indicate that these well-defined inorganic particles can be used as acceptor materials for the P3HT donor. Clusters 3 and 4 showed improved quenching ability over 5 due to their thienyl moiety increasing interfacial interactions between the polymer and the clusters. AFM shows improved interaction between the thienyl ligand containing clusters (3 and 4) and P3HT is observed when compared to 5. The improved interaction between the clusters and P3HT compared to traditional nanoparticles can be attributed to the incorporation of the thienyl moiety on the cluster. Increasing the

number of aromatic groups on the phosphine also increases the intermolecular interactions of the cluster, which provide the clusters with the ability to form ordered networks throughout the polymer film.

The combination of optimal orbital overlap and network formation make these clusters exciting materials for new organic-inorganic hybrid applications. The functionalized ligands in the cluster open the possibility of polymerization directly from the metal cluster, which could lay the foundation for covalently linked organic-inorganic hybrid systems. Continuing work includes the exploration of solution processed BHJ devices as well as developing copolymerization conditions for these clusters and 3-hexylthiophene.

## Acknowledgements

The authors are grateful to Research Corporation (Cottrell College Science Award 22628 and Development Award 7957), NSF (Research Experience for Undergraduates Grant 1062629) and the James Madison University Department of Chemistry and Biochemistry for financial support. The authors would also like to thank Dr. Kyle Plunkett for cyclic voltammetry data collection and Dr. Mark Dante for useful discussions about AFM.

## Notes and references

- 1 W. J. E. Beek, M. M. Wienk, and R. A. J. Janssen, *J. Mat. Chem.*, 2005, **15**, 2985.
- 2 W. J. E. Beek, M. M. Wienk, M. Kemerink, X. Yang, and R. A. J. Janssen, *J. Phys. Chem. B*, 2005, **109**, 9505.
- 3 C. Borriello, S. Masala, V. Bizzarro, G. Nenna, M. Re, E. Pesce, C. Minarini, and T. DiLuccio, *J. App. Polym. Sci.*, 2011, **122**, 3624.
- 4 E. Maier, A. Fischereder, W. Haas, G. Mauthner, J. Albering, T. Rath, F. Hofer, E. J. W. List, and G. Trimmel, *Thin Solid Films*, 2011, **519**, 4201.
- 5 J. Seo, M. J. Cho, D. Lee, A. N. Cartwright, and P. N. Prasad, *Adv. Mater.*, 2011, **23**, 3984.
- 6 R. J. Tseng, J. Huang, J. Ouyang, R. B. Kaner, and Y. Yang, *Nano Lett.* 2005, **5**, 1077.
- 7 J. Ouyang, C.-W. Chu, D. Sieves, and Y. Yang, *Appl. Phys. Lett.* 2005, **86**, 123507.
- 8 J. H. Park, Y. T. Lim, O. O. Park, K. Jai, J. K. Kim, J.-W. Yu, and Y. C. Kim, *Chem. Mater.*, 2004, **16**, 688.
- 9 G. D. Hale, J. B. Jackson, O. E. Shmakova, T. R. Lee, and N. J. Halas, *Appl. Phys. Lett.* 2001, **78**, 1502.

- 10 C. Lamy and J.-M. Leger, "Catalysis and Electrocatalysis at Nanoparticle Surfaces," ed. A. Wieckowski, E. R. Savinova, and C. G. Vayenas, Marcel Dekker, New York, N.Y., 2003.
- 11 W. C. Yen, Y. H. Lee, J. F. Lin, C. A. Dai, U. S. Jeng, and W. F. Su, *Langmuir*, 2011, **27**, 109.
- 12 I. Gur, N. A. Fromer, C.-P. Chen, A. G. Kanaras, and A. P. Alivisatos, *Nano Lett.*, 2007, **7**, 409.
- 13 S. Dayal, M. O. Reese, A. J. Ferguson, D. S. Ginley, C. Rumbles, and N. Kopidakis, *Adv. Funct. Mater.*, 2010, **20**, 2629.
- 14 M. A. Breimer, G. Yevgeny, S. Sy, and O. A. Sadik, *Nano Lett.* 2001, **1**, 305.
- 15 T. K. Sarma, D. Chowdhury, A. Paul, and A. Chattopadhyay, *Chem. Commun.* 2002, **35**, 1048.
- 16 L. Zhai, and R. D. McCullough, *J. Mater. Chem.* 2004, **14**, 141.
- 17 W.U. Huynh, J.J. Dittmer, and A.P. Alivisatos, *Science* 2002, **295**, 2425.
- 18 W.U. Huynh, X. Peng, and A. P. Alivisatos, *Adv. Mater.* 1999, **11**, 923.
- 19 D. Aldakov, T. Jiu, M. Zagorska, R. D. Bettignies, P. H. Jouneau, A. Pron, and F. Chandezon, *Phys. Chem. Chem. Phys.*, 2010, **12**, 7497.
- 20 O. P. Dimitriev, N. A. Ogurtsov, Y. Li, A. A. Pud, G. Gigli, P. S. Piryatinski, Y. V. Noskov, and A. S. Kutsenko, *Colloid. Polym. Sci.*, 2012, **290**, 1145.
- 21 R. Jetson, K. Yin, K. Donovan, and Z. Zhu, *Mater. Chem. Phys.*, 2010, **124**, 417.
- 22 N. Tomczak, D. Janczewski, M. Han, and G. J. Vancso, *Progress in Polymer Science (Oxford)*, 2009, **34**, 393.
- 23 L. Lokteva, N. Radychev, F. Witt, J. P. Borchert, and J. Kolny-Olesiak, *J. Phys. Chem. C.*, 2010, **114**, 12784.
- 24 J. E. Kroeze, T. J. Savenije, M. J. W. Vermeulen, and J. M. Warman, *J. Phys. Chem.*, 2003, **107**, 7696.
- 25 P. E. Shaw, A. Ruseckas, and I. D. W. Samuel, *Adv. Mater.*, 2008, **20**, 3516.
- 26 G. Keglevich, *Organophosphorous Chemistry* 42, Royal Society of Chemistry, 2013, 49.
- 27 M.L. Steigerwald, T. Siegrist, and S.M. Stuczynski, *Inorg. Chem.*, 1991, **30**, 4940.
- 28 S.M. Stuczynski, Y-U. Kwon, and M.L. Steigerwald, *J. Organomet. Chem.*, 1993, **449**, 167.
- 29 C.M. Evans, L.C. Class, K.E. Knowles, D.B. Tice, R.P.H. Chang, and E.A. Weiss, *J. Coord. Chem.*, 2012, **65**, 2391.
- 30 H. Liu, J.S. Owen, A.P. Alivisatos, *J. Am. Chem. Soc.*, 2007, **129**, 305.
- 31 A.G. Algarra, M. G. Basallote, M. J. Fernandez-Trujillo, E. Guillamon, R. Llusar, M. D. Segarra, and C. Vincent, *Inorg. Chem.*, 2007, **46**, 7668.
- 32 M. N. Sokolov, A. V. Anyushin, A. V. Virovets, I. V. Mirzaeva, N. F. Zakharchuk, and V. P. Fedin, *Inorg. Chem. Comm.*, 2011, **14**, 1659.
- 33 A. V. Anyushin, M. N. Skolov, A. V. Virovets, N. F. Zakharchuk, D. A. Mainichev, and V. P. Fedin, *Inorg. Chem. Comm.*, 2012, **24**, 225.
- 34 S. Perruchas, S. Flores, B. Jousseme, E. Lobkovsky, H. Abruña, F.J. DiSalvo, *Inorg. Chem.* 46 (2007) 8976-8987.
- 35 B. M. Boardman, J. R. Widawsky, Y. S. Park, C. L. Schenck, L. Venkataraman, M.L. Steigerwald, and C. Nuckolls, *J. Am. Chem. Soc.*, 2011, **133**, 8455.
- 36 Q. Wang, R. Takita, Y. Kikuzaki, and F. Ozawa, *J. Am. Chem. Soc.* 2010, **132**, 11420.
- 37 T. M. Pappenfus, D. L. Hermanson, S. G. Kohl, J. H. Melby, L. M. Thoma, N. E. Carpenter, D. A. da Silva Filho, and J.-L. Bredas, *J. Chem. Ed.*, 2010, **87**, 522.
- 38 B. J. Reeves and B. M. Boardman, *Polyhedron*, 2014, **73**, 118.
- 39 X. Roy, C. L. Schenck, S. Ahn, R. A. Lalancette, L. Venkataraman, C. Nuckolls, and M.L. Steigerwald, *Angew. Chem. Int. Ed.*, 2012, **51**, 12473.
- 40 Y. Li, *Acc. Chem. Res.* 2011, **44**, 723.
- 41 J. Hou, Z. Tan, Y. Yan, Y. He, C. Yang, Y. Li, *J. Am. Chem. Soc.* 2006, **128**, 4911.
- 42 Y. He, Y. Li, *Phys. Chem. Chem. Phys.* 2011, **13**, 1970.
- 43 W. U. Huynh, X. Peng, and A. P. Alivisatos, *Adv. Mater.*, 1999, **11**, 923.
- 44 B.C Sih, and M. O. Wolf, *J. Phys. Chem. C*, 2007, **111**, 17184.
- 45 M. Dante, J. Peet, and T.-C. Nguyen, *J. Phys. Chem. C.*, 2008, **112**, 7241.

In progress towards a covalently linked organic-inorganic structure, cobalt chalcogenide clusters were synthesized with thienyl phosphines ligands. Results indicate the clusters have potential as new acceptor materials for P3HT.

